BUTTERWORTH HEINEMANN

The flux integral method for multidimensional convection and diffusion

B. P. Leonard

Center for Computational Mechanics, The University of Akron, Akron, OH, USA

M. K. MacVean and A. P. Lock

Atmospheric Processes Research Division, Meteorological Office, Bracknell, Berkshire, UK

The flux integral method is a procedure for constructing an explicit single-step forward-in-time conservative control-volume update of the unsteady multidimensional convection–diffusion equation. The convective-plus-diffusive flux at each face of a control-volume cell is estimated by integrating the transported variable and its face-normal derivative over the volume swept out by the convecting velocity field. This yields a unique description of the fluxes, whereas other conservative methods rely on nonunique, arbitrary pseudoflux-difference splitting procedures. The accuracy of the resulting scheme depends on the form of the subcell interpolation assumed, given cell-average data. Cellwise constant behavior results in a (very artificially diffusive) first-order convection scheme. Second-order convection–diffusion schemes correspond to cellwise linear (or bilinear) subcell interpolation. Cellwise quadratic subcell interpolants generate a highly accurate convection–diffusion scheme with excellent phase accuracy. Under constant coefficient conditions, this is a uniformly third-order polynomial interpolation algorithm (UTOPIA).

Keywords: flux integral, convection, advection, control volume, higher order, multidimensional, conservative, UTOPIA

1. The flux integral

Consider the cell-average value of the transported scalar, $\bar{\phi}$, at a reference (central) cell, C. In two dimensions, an *exact* single-step explicit update can be written for the "new" (superscript +) cell value:

$$\bar{\phi}_C^+ = \bar{\phi}_C + \mathrm{FLUX}_w(i,j) - \mathrm{FLUX}_w(i+1,j) + \mathrm{FLUX}_s(i,j) - \mathrm{FLUX}_s(i,j+1) \quad (1)$$

using standard index and compass-point notation. Note that this is strictly conservative in that the east-face convective-plus-diffusive flux of cell C, at (i,j), is identical to the west-face flux at $(i+1,j)$; similarly for the north- and south-face fluxes. In equation (1), the west-face flux, for example, is given by

$$\mathrm{FLUX}_w(i,j) = \langle c_{xw}\phi_w \rangle - h\left\langle \alpha_w \left(\frac{\partial \phi}{\partial x}\right)_w \right\rangle \quad (2)$$

where the angle brackets represent *time averages* over Δt, and, assuming (for convenience) a uniform square mesh of side h, the west-face normal-component Courant number is

$$c_{xw} = \frac{u_w(t)\Delta t}{h} \quad (3)$$

and the west-face nondimensional diffusion parameter is written in terms of the (scalar) diffusivity, D_w, as

$$\alpha_w = \frac{D_w(t)\Delta t}{h^2} \quad (4)$$

with analogous definitions for the south face.

The convective contribution in equation (2) is equivalent to the total "mass" of ϕ swept through the west face along particle paths (or streamlines, in steady flow) over Δt. In principle, one could trace the particle paths backward to the earlier time level, for each face. This is shown, schematically, in *Figure 1*. Then the (exact) purely convective contribution is equivalent to integrating $\phi(x, y)$ *at the earlier time level* over the area (or volume, in three dimensions) swept out by the particle paths:

$$\langle c_{xw}\phi_w \rangle = \iint_{\mathrm{PPA}} \phi(x, y)\, d(x/h)\, d(y/h) \quad (5)$$

where PPA stands for particle path area.

The flux integral method now approximates equation (5) by replacing the particle path area by the flux integral

Address reprint requests to Prof. B. P. Leonard at the Center for Computational Mechanics, The University of Akron, Akron, OH 44325, USA.

Received 1 June 1994; revised 15 December 1994; accepted 16 January 1995

655 Avenue of the Americas, New York, NY 10010

0307-904X/95/$10.00
SSDI 0307-904X(95)00017-E

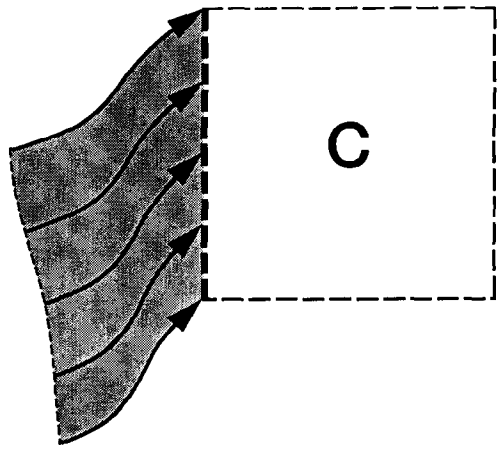

Figure 1. Schematic drawing of particle paths flowing into the west face of cell *C* is shown.

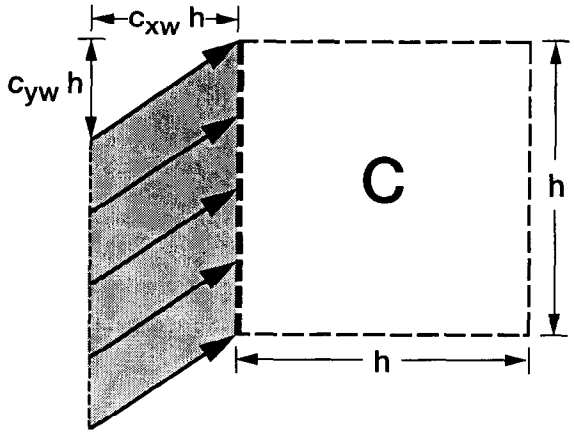

Figure 2. The flux integral parallelogram in the vicinity of the west face of cell *C*. c_{xw}, $c_{yw} > 0$.

parallelogram (FIP) by assuming the convecting velocity field to be locally constant (in both space and time) in the vicinity of the face in question. This is shown in *Figure 2*; note that the parallelogram is defined by the local (space-time-averaged) Courant number components, c_{xw} and c_{yw} (taken as both positive in the case shown). The flux integral convective approximation is thus

$$\langle c_{xw}\phi_w \rangle \approx \iint_{\text{FIP}} \phi(x, y)\, d(x/h)\, d(y/h) \tag{6}$$

A similar approximation for the diffusive contribution results in

$$-h\left\langle \alpha_w \left(\frac{\partial \phi}{\partial x}\right)_w \right\rangle \approx -\frac{\alpha_w h}{c_{xw}} \iint_{\text{FIP}} \frac{\partial \phi}{\partial x}\, d(x/h) d(y/h) \tag{7}$$

where α_w is an appropriate average. If the subcell behavior at the earlier time level, $\phi(x, y)$, were known in complete detail, equation (6) would represent an exact flux due to pure convection by a constant velocity field. For nonzero diffusion, it turns out that equation (7) represents the diffusive flux to third order, provided the subcell behavior is known in enough detail. The major task in the flux integral method is thus an interpolation problem:

Given a set of cell-average values, estimate subcell behavior in an accurate (and, ideally, shape-preserving) manner, while observing the cell-average constraint:

$$\iint_{\text{cell}} \phi(x, y)\, d(x/h)\, d(y/h) = \bar{\phi}_{\text{cell}} \text{ for all cells} \tag{8}$$

with an analogous formula in three dimensions.

For constant-density flow, the face-normal component Courant numbers used in constructing the flux integral parallelograms should satisfy a discrete continuity equation for each cell:

$$c_{xw}(i, j) - c_{xw}(i + 1, j) + c_{ys}(i, j) - c_{ys}(i, j + 1) = 0 \tag{9}$$

Since the area of a flux integral parallelogram is proportional to the face-*normal* Courant number component (e.g., the shaded area in *Figure 2* is $c_{xw}h^2$), an initially constant scalar field will remain constant everywhere (to machine accuracy). This can be seen in *Figure 3*, where the sum of the "inflow areas" equals the sum of the "outflow areas" (irrespective of the local individual face-*transverse* Courant number components). The appearance of "overlapping" characteristics in *Figure 3* should be no cause for concern. The important thing to note is that the spatial extent of characteristics passing through any given face is uniquely defined.

In the following sections, a number of different subcell interpolants are explored. A cellwise constant interpolant (locally equal to the cell average) results in a (very artificially diffusive) first-order convection scheme; modelled physical diffusion is absent, to a consistent order. This is not a viable scheme for practical CFD calculations. But, because of its simplicity, it is instructive to explore the flux integral method in this case. Bilinear

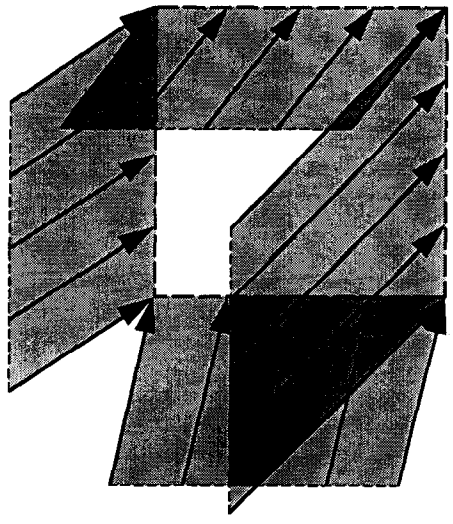

Figure 3. Flux integral parallelograms on each face of cell *C*.

downwind-weighted subcell interpolation results in a two-dimensional analog of the Lax–Wendroff scheme.[1] A cellwise quadratic interpolant over each cell generates a convection–diffusion scheme that is formally third-order accurate under constant coefficient conditions. These three methods are briefly compared using the well-known "rotating hill" test problem.

2. First-order convection

Fluxes will be calculated for the west face of cell C. Entirely analogous fluxes for the south face can be written down using appropriate (x, y) permutations. Unless otherwise noted, the Courant number components will be taken as both positive. Referring to *Figure 4*, the west-face convective flux integral corresponding to equation (6) can be thought of as consisting of a combination of three separate integrals

$$\mathrm{FLUX}_w(i,j) = I_1 - I_2 + I_3 \tag{10}$$

where I_1 is the integral over the rectangular area, 12461, in cell W; I_2 is over the triangular area, 1231, in cell W; and I_3 is over a similar triangular area, 6456, in cell SW. Assuming ϕ to be cellwise constant (equal to the respective cell average), the integrals in equation (1) are proportional to the respective areas times the local cell average value. This gives a first-order FIM of

$$\mathrm{FLUX}_w(i,j) = c_{xw}\bar{\phi}_W - \frac{c_{xw}c_{yw}}{2}\bar{\phi}_W + \frac{c_{xw}c_{yw}}{2}\bar{\phi}_{SW} \tag{11}$$

or, on rearrangement,

$$\mathrm{FLUX}_w(i,j) = c_{xw}\left[\bar{\phi}_W - \frac{c_{yw}}{2}(\bar{\phi}_W - \bar{\phi}_{SW})\right] \tag{12}$$

The term in square brackets can be considered the effective average convected face value. Note that it consists of the one-dimensional, first-order upwind ("donor-cell") value, $\bar{\phi}_W$, modified by a *transverse gradient* term proportional to the transverse Courant number component at the face. It should be clear how the formula changes for other combinations of signs of c_{xw} and c_{yw}. To a consistent order, there is no (physical) diffusive flux, since cellwise constant behavior implies a zero gradient within each cell.

Substituting equation (12) and the analogous formula for FLUX_s into equation (1) gives an overall (constant coefficient) convective update equation:

$$\bar{\phi}_C^+ = \bar{\phi}_C - c_x(\bar{\phi}_C - \bar{\phi}_W) - c_y(\bar{\phi}_C - \bar{\phi}_S) + c_x c_y(\bar{\phi}_C - \bar{\phi}_W - \bar{\phi}_S + \bar{\phi}_{SW}) \tag{13}$$

This is identical to a semi-Lagrangian update,[2] using *bilinear* interpolation around the departure point, collocated at *node* values: $\bar{\phi}_C$, $\bar{\phi}_W$, $\bar{\phi}_{SW}$, and $\bar{\phi}_S$ (located at the centroids of the respective cells). (For cellwise constant, linear, or bilinear interpolants, node values are equal to the respective cell average values. This is *not* the case for higher order interpolants.)

Using an appropriate upwinding strategy for other convecting velocity directions, it is not hard to show that the von Neumann stability condition for this scheme is given by a square region in the (c_x, c_y) plane:

$$|c_x| \le 1 \quad \text{and} \quad |c_y| \le 1 \tag{14}$$

3. Second-order methods

Second-order convection–diffusion methods result from assuming cellwise linear or bilinear subcell behavior. In this case, it is convenient to introduce local, normalized coordinates in cell W:

$$\xi = \frac{x}{h} - (i-1) \tag{15}$$

and

$$\eta = \frac{y}{h} - j \tag{16}$$

as shown in *Figure 5*. Note that the central cell, C, is located at (i, j). The top of the flux integral parallelogram (line $3 \rightarrow 1$ in *Figure 4*) is represented by

$$\eta_{\mathrm{top}}(\xi) = 0.5 + \frac{c_{yw}}{c_{xw}}(\xi - 0.5) \tag{17}$$

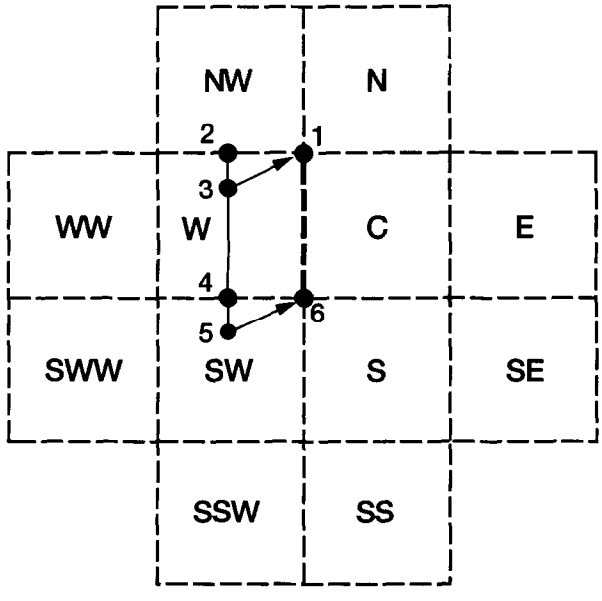

Figure 4. Twelve cells in the vicinity of the west face of cell C. c_{xw}, $c_{yw} > 0$.

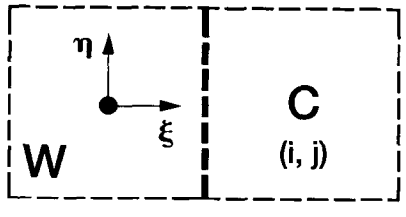

Figure 5. Definition of local normalized coordinates within cell W.

A general bilinear subcell interpolant within cell W takes the form

$$\phi(\xi, \eta) = C_1 + C_2\xi + C_3\eta + C_4\xi\eta \tag{18}$$

The cell-average constraint, equation (8), implies that

$$C_1 = \bar{\phi}_W \tag{19}$$

The slope constants, C_2 and C_3, and the twist constant, C_4, can be chosen in a number of different ways. For example, a two-dimensional analog of Fromm's method[3] results from choosing

$$C_2 = \frac{1}{2}(\bar{\phi}_C - \bar{\phi}_{WW}) \tag{20}$$

$$C_3 = \frac{1}{2}(\bar{\phi}_{NW} - \bar{\phi}_{SW}) \tag{21}$$

and

$$C_4 = 0 \tag{22}$$

Note that this involves a symmetrical node distribution with respect to cell W, independent of the velocity direction. Upwind or downwind weighting can also be used. In the interest of brevity, only one second-order scheme will be considered here in detail. This is based on *downwind*-weighted *bilinear* interpolation. For example, throughout cell W, the interpolant is collocated (for c_{xw}, $c_{yw} > 0$) at *node* values: $\bar{\phi}_C$, $\bar{\phi}_N$, and $\bar{\phi}_{NW}$ (in addition to ϕ_W). This turns out to be a two-dimensional generalization of the Lax–Wendroff method. For positive Courant number components, the interpolant within cell W is

$$\phi(\xi, \eta) = \bar{\phi}_W + (\bar{\phi}_C - \bar{\phi}_W)\xi + (\bar{\phi}_{NW} - \bar{\phi}_W)\eta + (\bar{\phi}_N - \bar{\phi}_{NW} - \bar{\phi}_C + \bar{\phi}_W)\xi\eta \tag{23}$$

with a corresponding normal gradient, within cell W,

$$\frac{\partial\phi}{\partial\xi} = (\bar{\phi}_C - \bar{\phi}_W) + (\bar{\phi}_N - \bar{\phi}_{NW} - \bar{\phi}_C + \bar{\phi}_W)\eta \tag{24}$$

Using local, cell-centered coordinates, similar formulas hold for each cell; in particular, cell SW formulas can be obtained from equations (23) and (24) by shifting all indexes "south" by one unit in equations (16), (23), and (24).

As before, the convective flux integral is split into three geometrically distinct parts, in this case,

$$I_1 = \int_{0.5-c_{xw}}^{0.5} \left[\int_{-0.5}^{0.5} \phi(\xi, \eta)\, d\eta \right] d\xi \tag{25}$$

$$= \int_{0.5-c_{xw}}^{0.5} [\bar{\phi}_W + (\bar{\phi}_C - \bar{\phi}_W)\xi]\, d\xi \tag{26}$$

$$= c_{xw}\bar{\phi}_W + \left(\frac{c_{xw} - c_{xw}^2}{2}\right)(\bar{\phi}_C - \bar{\phi}_W) \tag{27}$$

When rearranged as

$$I_1 = c_{xw}\left[\frac{1}{2}(\bar{\phi}_C + \bar{\phi}_W) - \frac{c_{xw}}{2}(\bar{\phi}_C - \bar{\phi}_W)\right] \tag{28}$$

this will be recognized as the *one-dimensional* Lax–Wendroff flux.[4] The second (negative) contribution over the triangular area in cell W is

$$-I_2 = -\int_{0.5-c_{xw}}^{0.5} \left[\int_{\eta_{top}(\xi)}^{0.5} \phi(\xi, \eta)\, d\eta \right] d\xi \tag{29}$$

Using equation (17), this becomes, after some rearrangement,

$$-I_2 = -c_{xw}c_{yw}\left[\begin{array}{l} \frac{1}{8}(\bar{\phi}_C + \bar{\phi}_W + \bar{\phi}_N + \bar{\phi}_{NW}) \\ -\frac{c_{xw}}{6}(\bar{\phi}_N + \bar{\phi}_C - \bar{\phi}_{NW} - \bar{\phi}_W) \\ -\frac{c_{yw}}{12}(\bar{\phi}_N + \bar{\phi}_{NW} - \bar{\phi}_C - \bar{\phi}_W) \\ +\frac{c_{xw}c_{yw}}{8}(\bar{\phi}_N - \bar{\phi}_{NW} - \bar{\phi}_C + \bar{\phi}_W) \end{array}\right] \tag{30}$$

Then, I_3 is obtained from I_2 by shifting all indexes south by one unit.

The diffusive flux is computed in a similar way. In particular

$$-\alpha_w\left(\frac{\partial\phi}{\partial\xi}\right)_{avg} = -\frac{\alpha_w}{c_{xw}}\iint_{FIP}\frac{\partial\phi}{\partial\xi}\, d\xi\, d\eta \tag{31}$$

This is also conveniently split into three parts. In this case

$$-\frac{\alpha_w}{c_{xw}} I_1 = -\alpha_w(\bar{\phi}_C - \bar{\phi}_W) \tag{32}$$

which will be recognized as the classical, second-order, *one-dimensional* expression for the diffusive flux across the west face. But there are also contributions from transverse convective coupling. In particular,

$$+\frac{\alpha_w}{c_{xw}} I_2 = \alpha_w\left[\begin{array}{l} \frac{c_{yw}}{4}(\bar{\phi}_N + \bar{\phi}_C - \bar{\phi}_{NW} - \bar{\phi}_W) \\ -\frac{c_{yw}^2}{6}(\bar{\phi}_N - \bar{\phi}_{NW} - \bar{\phi}_C + \bar{\phi}_W) \end{array}\right] \tag{33}$$

and the corresponding I_3 term is again obtained by shifting all indexes south by one unit.

The total west-face convective-plus-diffusive flux is:

BILINEAR DOWNWIND

$$\mathrm{FLUX}_w(i,j) = c_{xw}\left\{\begin{array}{l}\frac{1}{2}(\bar\phi_C+\bar\phi_W)-\frac{c_{xw}}{2}(\bar\phi_C-\bar\phi_W)\\ -\frac{c_{yw}}{8}[(\bar\phi_N-\bar\phi_S)+(\bar\phi_{NW}-\bar\phi_{SW})]\\ +\frac{c_{xw}c_{yw}}{6}[(\bar\phi_N-\bar\phi_S)-(\bar\phi_{NW}-\bar\phi_{SW})]\\ +\frac{c_{yw}^2}{12}[(\bar\phi_N-2\bar\phi_C+\bar\phi_S)+(\bar\phi_{NW}-2\bar\phi_W+\bar\phi_{SW})]\\ -\frac{c_{xw}c_{yw}^2}{8}[(\bar\phi_N-2\bar\phi_C+\bar\phi_S)-(\bar\phi_{NW}-2\bar\phi_W+\bar\phi_{SW})]\end{array}\right\}$$

$$-\alpha_w\left\{\begin{array}{l}(\bar\phi_C-\bar\phi_W)-\frac{c_{yw}}{4}[(\bar\phi_N-\bar\phi_S)-(\bar\phi_{NW}-\bar\phi_{SW})]\\ +\frac{c_{yw}^2}{6}[(\bar\phi_N-2\bar\phi_C+\bar\phi_S)-(\bar\phi_{NW}-2\bar\phi_W+\bar\phi_{SW})]\end{array}\right\} \tag{34}$$

The interesting feature of this formula is that (referring to *Figure 4*) every term is face-centered in both the x and y directions. In this case, the *downwind-weighted* subcell interpolation is "balanced" by the *natural upwinding* involved in the flux integral calculation. The resulting convective-plus-diffusive flux is independent of the velocity direction, just like the Lax–Wendroff method in one dimension. The overall update equation involves the square, nine-point stencil, centered on C. For pure convection at constant velocity, the update is identical to that of a semi-Lagrangian scheme using a biquadratic polynomial collocated at the same nine-point stencil.

Although the semi-Lagrangian convection scheme can be obtained from the flux-integral form, the reverse is not true. This is easily seen by writing out the complete update based on equation (34). Notice how the $c_x(c_xc_y)$ term from the east–west flux difference combines with the $c_y(c_x^2)$ term from the north–south flux difference. The purely convective von Neumann stability region is again the square, given by equation (14). Stability regions in the (c_x, c_y) plane for finite values of α have been established and will be discussed in a separate article.

4. Uniformly third-order polynomial interpolation algorithm, UTOPIA

Assuming a velocity-direction-independent cellwise *quadratic* subcell interpolation within each cell leads to a polynomial interpolation algorithm for convection and diffusion that is uniformly third-order accurate under constant-coefficient conditions. In a variable (but solenoidal) convecting velocity field, with possibly variable diffusivity, the algorithm is no longer formally third-order accurate; however, the practical accuracy is significantly better than that of formally second-order schemes. Phase accuracy, in particular, is excellent, just as in the case of the corresponding one-dimensional QUICKEST scheme.[5–7]

Within cell W, the quadratic interpolation takes the (velocity-direction-independent) form:

$$\begin{aligned}\phi(\xi,\eta) = {}& \bar\phi_W-\frac{1}{24}(\bar\phi_C+\bar\phi_{SW}+\bar\phi_{WW}+\bar\phi_{NW}-4\bar\phi_W)\\ &+\left(\frac{\bar\phi_C-\bar\phi_{WW}}{2}\right)\xi+\left(\frac{\bar\phi_C-2\bar\phi_W+\bar\phi_{WW}}{2}\right)\xi^2\\ &+\left(\frac{\bar\phi_{NW}-\bar\phi_{SW}}{2}\right)\eta+\left(\frac{\bar\phi_{NW}-2\bar\phi_W+\bar\phi_{SW}}{2}\right)\eta^2\end{aligned} \tag{35}$$

Note that this satisfies the cell-average constraint of equation (8). Also note that the nodal value, ϕ_W, is not the same as the cell average; in fact,

$$\begin{aligned}\phi_W &= \phi(0,0)\\ &= \bar\phi_w-\frac{1}{24}(\bar\phi_C+\bar\phi_{SW}+\bar\phi_{WW}+\bar\phi_{NW}4\bar\phi_W)\end{aligned} \tag{36}$$

The x-direction gradient within cell W is

$$\frac{\partial\phi}{\partial\xi} = \left(\frac{\bar\phi_C-\bar\phi_{WW}}{2}\right)+(\bar\phi_C-2\bar\phi_W+\bar\phi_{WW})\xi \tag{37}$$

4.1 *Convective flux in the absence of diffusion*

For pure convection, the west-face flux is computed in the usual way. As is perhaps by now expected, the first component of the flux integral generates the one-dimensional (in this case, QUICKEST) formula:

$$\begin{aligned}I_1 = c_{xw}\Big[&\frac{1}{2}(\bar\phi_C+\bar\phi_W)-\frac{c_{xw}}{2}(\bar\phi_C-\bar\phi_W)\\ &-\left(\frac{1-c_{xw}^2}{6}\right)(\bar\phi_C-2\bar\phi_W+\bar\phi_{WW})\Big]\end{aligned} \tag{38}$$

Note the appearance of the upwind-weighted normal-curvature term (resulting from the natural upwinding

inherent in the flux integral). Integration over the respective triangular areas in cells W and SW introduces several cross-difference terms. The final form of the purely convective flux is (referring to *Figure 4*)

QUADRATIC (CONVECTION)

$$\mathrm{FLUX}_w(i,j) = c_{xw}\left\{\begin{array}{l} \frac{1}{2}(\bar{\phi}_C + \bar{\phi}_W) - \frac{c_{xw}}{2}(\bar{\phi}_C - \bar{\phi}_W) \\ \qquad -\left(\frac{1-c_{xw}^2}{6}\right)(\bar{\phi}_C - 2\bar{\phi}_W + \bar{\phi}_{WW}) \\ -\frac{c_{yw}}{2}(\bar{\phi}_W - \bar{\phi}_{SW}) \\ -c_{yw}\left(\frac{1}{4} - \frac{c_{xw}}{3}\right)(\bar{\phi}_C - \bar{\phi}_W - \bar{\phi}_S + \bar{\phi}_{SW}) \\ -c_{yw}\left(\frac{1}{4} - \frac{c_{yw}}{6}\right)(\bar{\phi}_{NW} - 2\bar{\phi}_W + \bar{\phi}_{SW}) \\ +c_{yw}\left(\frac{1}{12} - \frac{c_{xw}^2}{8}\right)\left[\begin{array}{l}(\bar{\phi}_C - 2\bar{\phi}_W + \bar{\phi}_{WW}) \\ -(\bar{\phi}_S - 2\bar{\phi}_{SW} + \bar{\phi}_{SWW})\end{array}\right] \\ +c_{yw}\left(\frac{1}{12} - \frac{c_{yw}^2}{24}\right)(\bar{\phi}_{NW} - 3\bar{\phi}_W + 3\bar{\phi}_{SW} - \bar{\phi}_{SSW})\Big] \end{array}\right\} \tag{39}$$

It is instructive to identify the role played by each of these terms. The first three terms represent the one-dimensional (QUICKEST) contribution; note that all the remaining terms contain a c_{yw} coefficient. The fourth term in equation (39) is the *transverse gradient* that previously appeared in the first-order scheme. This is, in fact, a second-order term, as is the *normal gradient* (second term). The fifth term represents *twist*, an interaction between normal and transverse convection. The next term is a *transverse-curvature* contribution. The final two terms in equation (39) are actually fourth-order contributions. Dropping these terms does not affect the formal (constant-coefficient) third-order accuracy of the overall update equation. However, they do affect the stability of the scheme. Without the higher-order terms, the purely convective stability region is *approximately* the diamond-shaped region

$$|c_x| + |c_y| < 1 \tag{40}$$

Including these terms (that arise naturally in the flux-integral formulation) results once again in the square stability region given by equation (14).

4.2 *Third-order diffusive flux*

Applying the usual three-part-integral procedure to equation (37) results in the following diffusive flux:

$$-\alpha_w\left(\frac{\partial\phi}{\partial\xi}\right)_{\mathrm{avg}} = -\alpha_w\left\{\begin{array}{l}(\bar{\phi}_C - \bar{\phi}_W) - \frac{c_{xw}}{2}(\bar{\phi}_C - 2\bar{\phi}_W + \bar{\phi}_{WW}) \\ -\frac{c_{yw}}{2}(\bar{\phi}_C - \bar{\phi}_W - \bar{\phi}_S + \bar{\phi}_{SW}) \\ +\frac{c_{xw}c_{yw}}{3}\left[\begin{array}{l}(\bar{\phi}_C - 2\bar{\phi}_W + \bar{\phi}_{WW}) \\ -(\bar{\phi}_S - 2\bar{\phi}_{SW} + \bar{\phi}_{SWW})\end{array}\right]\end{array}\right\} \tag{41}$$

The first term is the classical (one-dimensional) second-order first-difference across the face. The second, *normal-curvature*, term represents the effect of normal convection on the time-averaged normal gradient; this is a third-order convection-diffusion cross-coupling term that also appears in the one-dimensional QUICKEST formula.[5] The third, twist, term represents the coupling effect of transverse convection; this is a (two-dimensional) third-order term. The final term is actually a (partial) fourth-order cross-coupling term, kept, once again, because of enhanced stability properties.

4.3 *Diffusive contribution to the convective flux*

The convection–diffusion coupling terms just described represent the effects of convection in estimating the diffusive flux. They arise naturally in the flux integral formulation. For uniformly third-order consistency, one also needs to estimate the analogous cross-coupling effects of diffusion on the convective flux.[5] Because of the assumed curvature in the subcell interpolation, diffusion changes the value of ϕ over Δt as it is being convected through a particular cell face. As shown in Ref. 8, this change is given by $(\alpha/2)\nabla^2\phi$. Performing the usual

three-part flux-integral calculation leads to an *additional diffusive* contribution to the convective flux of the form

$$c_{xw}\left\{\begin{array}{l}\dfrac{\alpha_w}{2}\left[(\bar{\phi}_C - 2\bar{\phi}_W + \bar{\phi}_{WW}) + (\bar{\phi}_{NW} - 2\bar{\phi}_W + \bar{\phi}_{SW})\right] \\ -\dfrac{\alpha_w c_{yw}}{4}\left[\begin{array}{l}(\bar{\phi}_C - 2\bar{\phi}_W + \bar{\phi}_{WW}) - (\bar{\phi}_S - 2\bar{\phi}_{SW} + \bar{\phi}_{SWW}) \\ +(\bar{\phi}_{NW} - 3\bar{\phi}_W + 3\bar{\phi}_{SW} - \bar{\phi}_{SSW})\end{array}\right]\end{array}\right\} \tag{42}$$

which must be added to equation (39) to give the total convective flux. The convective-plus-diffusive flux at the west face is thus the sum of equations (39), (41), and (42). A von Neumann stability analysis of the constant-coefficient overall update algorithm shows that the useful region in (c_x, c_y, α) space is given, as a minimum, by the "cylinder":

$$|\mathbf{c}| \leq 1, \qquad 0 \leq \alpha \leq 0.25 \tag{43}$$

5. Comparison with other methods

Because fluxes are estimated directly, (for a given subcell interpolation) the flux integral method produces unique formulas for the fluxes. This is in contrast to other methods that have been used to construct *conservative* multidimensional convection (or convection–diffusion) schemes. For example, Ekebjærg and Justesen[9] developed a nominally third-order, two-dimensional convection–diffusion scheme by successive elimination of truncation error terms arising from a lower-order scheme. The nonconservative single-step explicit update was then rewritten in a conservative pseudoflux-difference form. But the pseudofluxes chosen by Ekebjærg and Justesen are not unique; except for first-order (and some simple second-order) schemes, there is, in general, no unique way of rewriting a nonconservative update in a conservative flux-difference form.

Recently, Rasch[10] has used, as a starting point, a (constant-coefficient) third-order semi-Lagrangian convection scheme, and then rewritten the update in conservative, pseudoflux-difference form. Recognizing the nonuniqueness problem, Rasch uses weighting parameters to generate a family of possible pseudoflux-difference algorithms. For certain choices of the weights, the (purely convective form of the) Ekebjærg-and-Justesen scheme can be retrieved. For other weights, Rasch's convection scheme is equivalent to (the convective part of) that used by the present authors in Ref. 8; this is also the form used by Rasch. For still other choices of the weights, a nominally third-order convective flux equivalent to equation (39)—but with the last two (higher-order) terms removed—can be obtained. The conservatively rewritten semi-Lagrangian approach does not generate diffusive fluxes.

In a very recent manuscript, LeVeque[11] has used a technique for purely convective flows similar, in some respects, to the flux integral method described here. For a constant convecting velocity field, LeVeque's Method V is a 10-point third-order two-dimensional convection scheme. This is the minimum number of points needed for third-order accuracy. The overall convective update is equivalent to the semi-Lagrangian scheme used as the starting point for Rasch's method; it is also equivalent to that of Ekebjærg and Justesen. LeVeque's Method VI is equivalent to the purely convective portion of the flux integral method developed here, i.e., equation (39). LeVeque does not consider diffusive fluxes.

6. Convective test problem

The three schemes described here have been applied to the rotating Gaussian hill problem under purely convective conditions ($\alpha = 0$). The convecting velocity field is that of solid-body rotation at an angular velocity of 0.2 rad/sec, with the axis at the center of a 61 × 61 square mesh. The Gaussian is initially centered at a point $15h$ above the center of rotation, with $\sigma = 3h$. *Figure 6* shows the initial state in a superfine-grid rendering. This is also the exact solution after an integral number of rotations. The cell-average initial data is shown in *Figure 7* as a two-dimensional histogram. The time step is chosen so that the maximum component Courant numbers (at the corners of the domain) are $\pi/10$. *Figure*

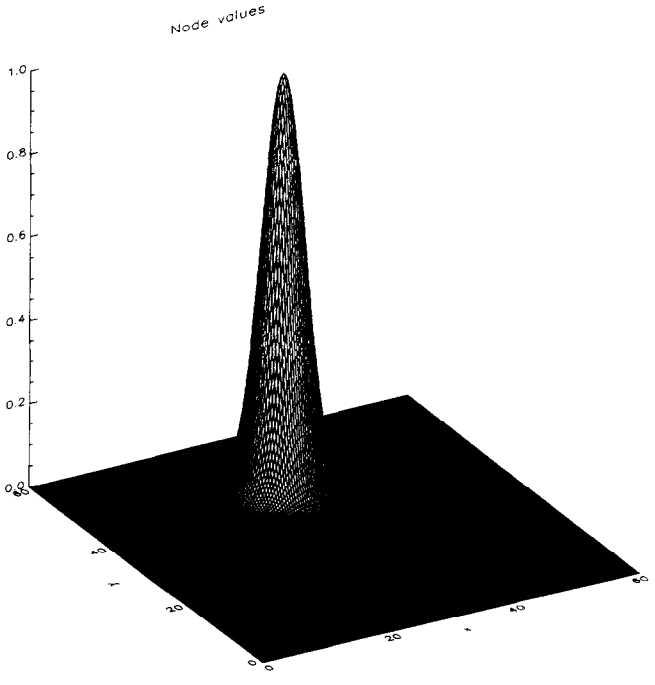

Figure 6. Initial Gaussian distribution, $\phi(x, y)$, shown on a very fine grid. This is also the exact (purely convective) solution after an integral number of rotations. $\phi_{max} = 1.000$.

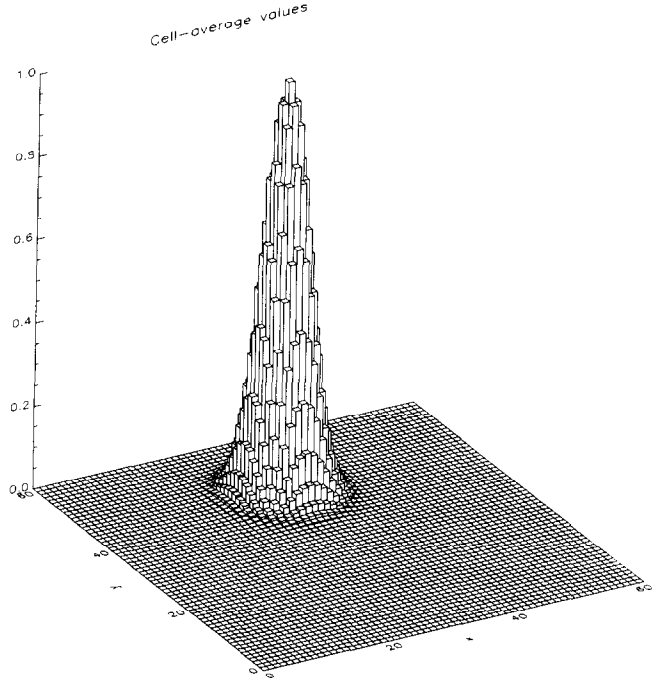

Figure 7. Initial state of cell-average values, $\bar{\phi}_{i,j}$ shown as a two-dimensional histogram on the 61 × 61 computational grid.

8 shows the first-order cell-average results after one (anticlockwise) rotation, or 600 time steps. This also represents the (piecewise constant) subcell interpolants. The "Lax–Wendroff" cell-average results are shown in *Figure 9*, with a close-up of the peak region, showing the (downwind-weighted) subcell behavior, in *Figure 10*. Note the discontinuities across cell faces and the change in behavior where c_y changes sign. *Figures 11* and *12* give the corresponding UTOPIA results.

As mentioned before, the first-order scheme is far too artificially diffusive to even be considered for practical application. As in one dimension, the Lax–Wendroff-type scheme is excessively dispersive, showing significant phase-lag errors in the "wake." By contrast, UTOPIA has good accuracy and excellent phase behavior, just as in the one-dimensional case.[5,7]

Other extensive studies of purely convective and convective–diffusive test problems at a number of grid refinements have consistently shown the superiority of UTOPIA. Not surprisingly, it is more accurate than lower-order schemes. It is also more expensive, *per mesh point calculation*. The important conclusion, however, is that, for a prescribed accuracy, UTOPIA can be used on a much coarser mesh (with a concomitantly larger time-step); *the overall cost is then much lower* than that of lower-order schemes.

6. Conclusion

The flux-integral method has been shown to be a useful technique for estimating genuinely multidimensional convective-plus-diffusive fluxes in a strictly conservative

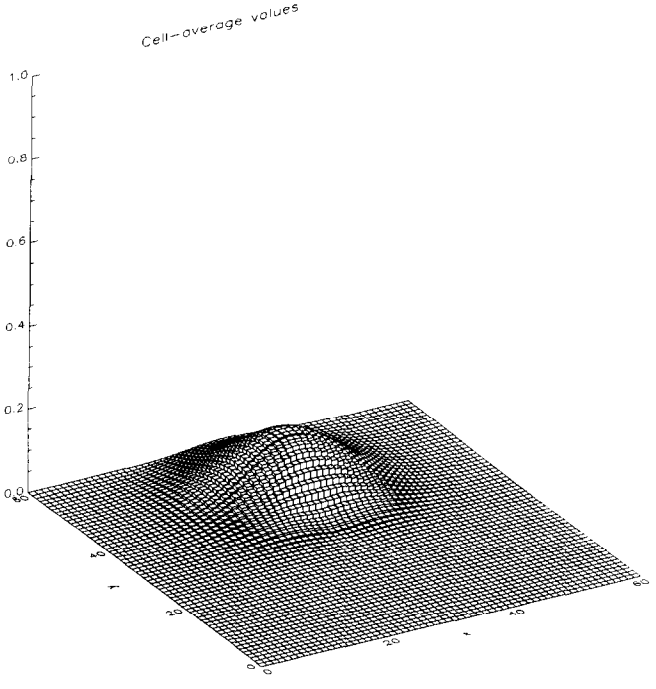

Figure 8. Solution after one (anticlockwise) rotation for the first-order method. In this case, the histogram of cell-average values also represents the cellwise constant subcell interpolation. $\bar{\phi}_{max} = 0.152$; $\bar{\phi}_{min} = 0.000$.

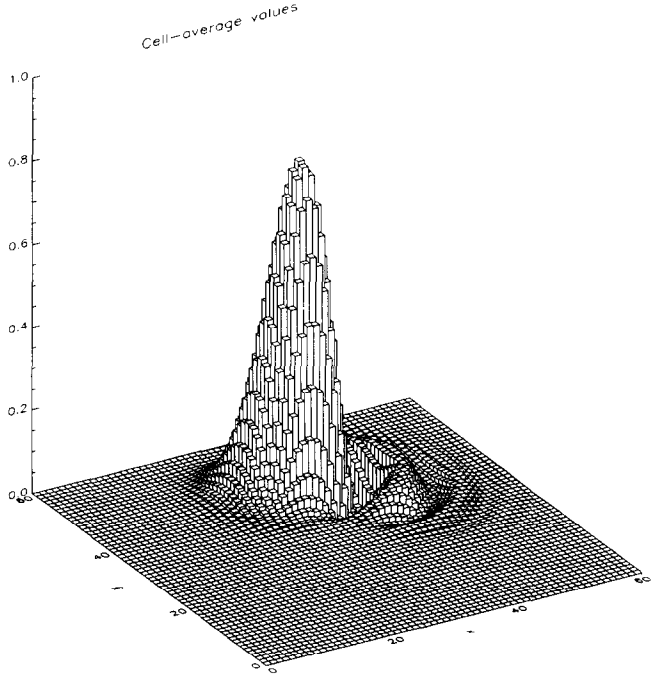

Figure 9. Solution of cell-average values after one rotation using the second-order convection scheme. $\bar{\phi}_{max} = 0.787$; $\bar{\phi}_{min} = -0.149$

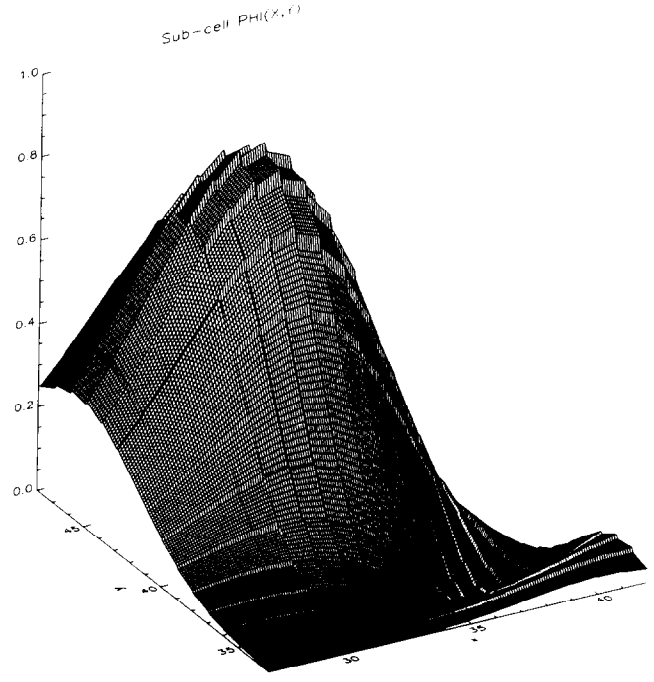

Figure 10. Close-up of the downwind-weighted bilinear subcell interpolation in the peak region, showing discontinuities across cell faces. $\phi_{max} = 0.823$; $\phi_{min} = -0.176$. The horizontal scales have been expanded by a factor of four in each direction

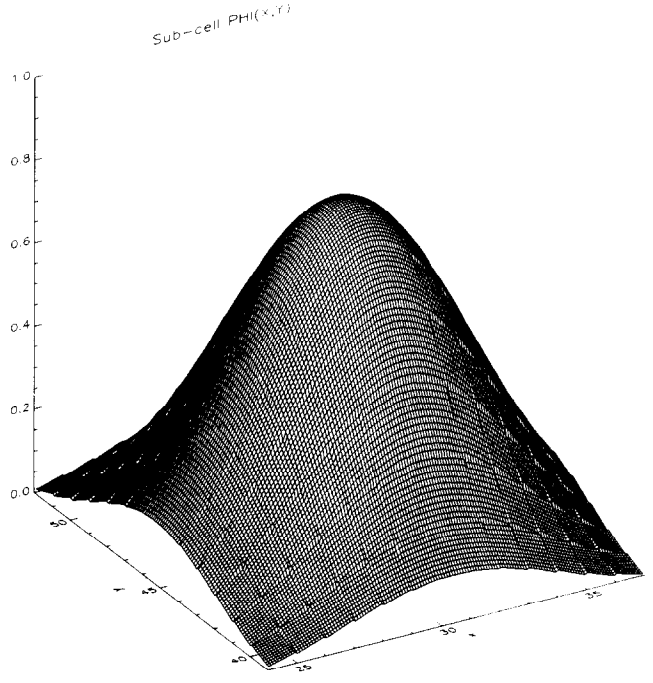

Figure 12. Close-up of the quadratic subcell interpolation in the peak region, showing (small) discontinuities across cell faces. $\phi_{max} = 0.810$; $\phi_{min} = -0.010$ (not shown). Same scale as *Figure 10*

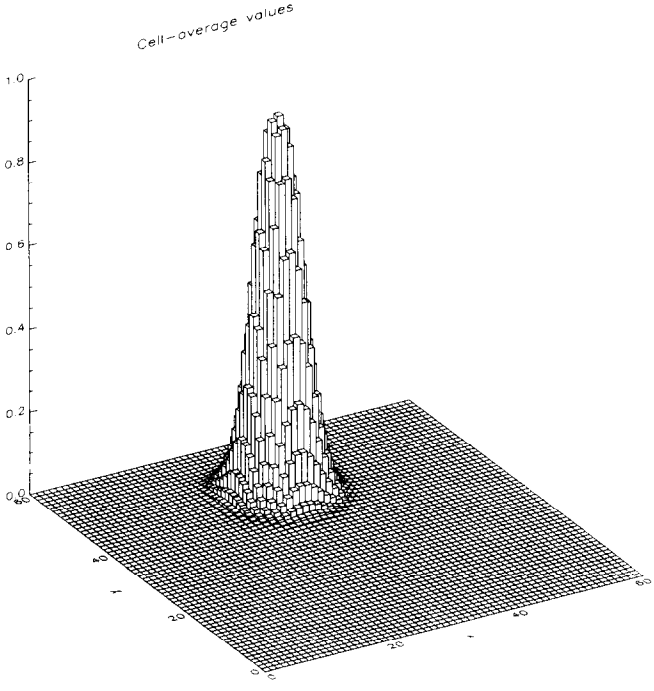

Figure 11. Solution of cell-average values after one rotation using the purely convective form of UTOPIA. $\bar{\phi}_{max} = 0.804$; $\bar{\phi}_{min} = -0.008$

formulation of an explicit, forward-in-time, single-step update formula. The assumption of locally constant convecting velocities near each control-volume face means that the formal accuracy of the convection terms is at most second order, e.g., the convecting velocity field could be staggered in time by $\Delta t/2$ with respect to transported scalars. Variable diffusivity would typically be lagged and therefore only first-order accurate in time. However, spatial accuracy is enhanced by using higher order subcell interpolation. Under constant-coefficient conditions, an Nth order subcell interpolation leads to an $(N + 1)$th order accurate convection–diffusion scheme in both space and time.

For the purely convective test problem considered here, the following conclusions can be drawn:

(1) Cellwise constant subcell interpolation leads to an unworkable (artificially diffusive) first-order convection scheme.
(2) Cellwise linear or bilinear interpolants generate second-order convection–diffusion schemes. Downwind-weighted bilinear interpolation gives a multidimensional analog of the Lax–Wendroff scheme. However, because of the velocity-direction–dependent weighting of the interpolant, this leads to a highly dispersive convection scheme with strong phase-lag errors, just as in one dimension.
(3) Cellwise quadratic interpolation (independent of velocity direction) leads to a very accurate convection–diffusion scheme with excellent phase behavior. Under constant coefficient conditions, this is a uniformly third-order polynomial interpolation algorithm (UTOPIA). Since highly accurate solutions can be obtained on relatively coarse grids, UTOPIA is much more cost-effective than lower-order methods.

For simplicity, the present paper has been confined to two dimensions. It should be clear that the flux integral

method generalizes to three dimensions in a straightforward manner. The technique can be used with even higher-order subcell interpolation (presumably using velocity-direction independent interpolants in order to minimize dispersion); higher order diffusive–diffusive and convective–diffusive cross-coupling terms are fairly complex but can be derived in a straightforward manner (e.g., using automatic symbolic manipulation). Further research is needed to extend the method to larger time steps. Finally, it should be pointed out that shape preservation in the subcell interpolation automatically results in a positivity preserving conservative multidimensional formulation, thus obviating the need for ad hoc flux-limiter constraints. This is an area of current research.

Acknowledgments

Most of this work was completed while the first author was a Visiting Research Scientist at the UK Meteorological Office. Portions of the first author's work were also supported by the Institute for Computational Mechanics in Propulsion (ICOMP) at the NASA Lewis Research Center in Cleveland, Ohio, under Space Act Agreement NCC 3-233, and by a National Science Foundation Mesoscale Meteorology Program grant ATM-9221808.

References

1 Lax, P. D. and Wendroff, B. Systems of conservation laws. *Comm. Pure Appl. Math.* 1960, **13**, 217–237
2 Staniforth, A. and Côté, J. Semi-lagrangian integration schemes—a review. *Monthly Weather Rev.* 1991, **119**, 2206–2223
3 Fromm, J. E. A method for reducing dispersion in convective difference schemes. *J. Comput. Phys.* 1968, **3**, 176–189
4 Leonard, B. P. Note on the von Neumann stability of explicit one-dimensional advection schemes. *Comput. Meth. Appl. Mech. Eng.* 1994, **118**, 29–46
5 Leonard, B. P. A stable and accurate convective modelling procedure based on quadratic upstream interpolation. *Comput. Meth. Appl. Mech. Eng.* 1979, **19**, 59–98
6 Leonard, B. P. Elliptic systems: finite-difference method IV. In: Minkowicz, W. J., Sparrow, E. M., Schneider, G. E. and Pletcher, R. H. (eds.). *Handbook of Numerical Heat Transfer.* Wiley, New York, 1988, 347–378
7 Leonard, B. P. The ULTIMATE conservative differencing scheme applied to unsteady one-dimensional advection. *Comp. Meth. Appl. Mech. Eng.* 1991, **88**, 17–74
8 Leonard, B. P., MacVean, M. K. and Lock, A. P. Positivity-preserving numerical schemes for multidimensional advection. 1993, NASA TM 106055, ICOMP-93-05, Lewis Research Center
9 Ekebjærg, L. and Justesen, P. An explicit scheme for advection-diffusion modelling in two dimensions. *Comp. Meth. Appl. Mech. Eng.* 1991, **88**, 287–297
10 Rasch, P. J. Conservative shape-preserving two-dimensional transport on a spherical reduced grid. *Monthly Weather Rev.* 1994, **122**, 1337–1350
11 LeVeque, R. J. High-resolution conservative algorithms for advection in incompressible flow. *SIAM J. Numer. Anal.*, in press